

CHAPTER 5

Potential model for collective group behaviour

We formulate a model for collective behaviour, based on principles from physical mechanics and particle physics. This model is based upon repulsion, attraction and alignment forces generated by group members and includes a dissipative force term. We shall analyse the components of the model and show that an alignment force is essential for inducing travel of the group, cohesive forces alone are not adequate.

5.1. Introduction

We consider an alternative way to model collective group behaviour, based upon social forces generated by the group members.

The concept of a force is essential to the development of physical mechanics. A force (\mathbf{F}) is a ‘push’ or ‘pull’ experienced by a mass when it is accelerated. In a conservative force field, the force on a body is given by the gradient of a potential (V) defined as $\mathbf{F} = -\nabla V$. Here, we define the direction differential operator (grad) on the function $V(x, y, z; t)$ as

$$\nabla V(x, y, z; t) = \frac{\partial V(x, y, z; t)}{\partial x} \hat{\mathbf{x}} + \frac{\partial V(x, y, z; t)}{\partial y} \hat{\mathbf{y}} + \frac{\partial V(x, y, z; t)}{\partial z} \hat{\mathbf{z}},$$

where $\hat{\mathbf{x}}$, $\hat{\mathbf{y}}$ and $\hat{\mathbf{z}}$ denote unit direction vectors. The magnitude of the vector differential operator ($|\nabla V(x, y, z; t)|$) is the maximum directional derivative. For a system of N particles, the force acting on the i -th particle is $\mathbf{F}_i = \sum_{j \neq i}^N \mathbf{F}_{ij} + \mathbf{F}_{external,i}$, where \mathbf{F}_{ij} are the internal forces acting on individual i resulting from the other group members and $\mathbf{F}_{external,i}$ are the external forces acting on individual i .

The attraction, alignment and repulsion forces in our potential model will be based on gradient forces (the motion of individuals follows the sum of the gradient of appropriate potentials). We will ignore external forces in our model. We introduce an alignment term designed to allow individuals to orient their velocities to one another. Our approach allows adoption of existing mathematical physics knowledge once we convert our Lagrangian system to an Eulerian approach (with Hamiltonian equations). There is a considerable body of work available on Hamiltonian mechanics, which can be used to analyse and further the study of this system.

Plasma theory is concerned with a state of matter which occurs when a gas is heated. A plasma is a gas consisting of charged and neutral particles, which exhibit collective behaviour. While the average

densities of the two types of particles in the plasma are similar, the individual particles are able to undergo (local) electromagnetic interactions (Chen 1984). A plasma has a sufficient amount of free charges for electromagnetic forces to be important to its macroscopic behaviour (Woods 2004, Nicholson 1983). We reinterpret these electromagnetic forces within the guise of social forces that an individual experiences. We will define a social potential energy function that encapsulates these social forces.

A gas is sufficiently diffuse for collisions involving three or more bodies to be neglected. The simplest model of a microscopic particle is a small uniform sphere, which has a spherically-symmetric force field. We shall preserve both of these assumptions (Woods 2004) when applying ideas of physical forces to the individuals within our system.

Models which use forces between individuals that are analogous to physical forces, have a long history. Parr (1927) proposed the idea of mutual interactions between individuals that are composed of attractions and repulsions, designed to maintain the group as a stable mass. Breder (1951) developed this idea further by discussing the possibility of modelling attraction forces between individual fish upon classical gravitation and electromagnetism. In a later paper, Breder (1954) considered inverse power laws to model the repulsions and attractions between individuals, with repulsion stronger at short inter-individual distances. Breder (1954) compared this model to actual fish schools, to obtain realistic values for model parameters. This article is one of the very first instances of the use of attraction and repulsion biological forces. Niwa (1994) uses a constant attraction force (unrealistic, but this does lead to a simpler mathematical treatment), coupled with an inverse square law repulsion. Exponential and power law forces were used to model social forces by Beecham & Farnsworth (1999). Beecham & Farnsworth's model [Beecham & Farnsworth (1999)] is considerably

more complicated than previous work, invoking foraging efficiency and predation risk to produce the social forces. Topaz, Bertozzi & Lewis (2005) use attractive and repulsive gradient force interactions, their model is based on interactions related to population density and not to the proximity of nearby neighbours. A differential equation is derived, based on this population density and Topaz et al. (2005) use this to examine macroscopic properties of clusters of individuals. The authors show that an equilibrium between the diffusion and attraction terms in their equation is able to cause the formation of clusters, given an initially disperse population. Topaz et al. (2005) do not include group motion in their formulation, their solutions are stationary ones only.

Flierl et al. (1999) introduce various models from physical literature, to examine biological aggregations. The authors transform an individual-based model into a continuum model, using a Fokker-Planck equation. This approach is useful for analysing global properties, but at the cost of losing track of individual social interactions.

Mogilner, Edelstein-Keshet, Bent & Spiros (2003) propose a Lagrangian model based on attractive and repulsive potentials, to investigate the spacing of individuals in a social aggregate. This is a different approach to an earlier paper, which uses an Eulerian approach (Mogilner & Edelstein-Keshet 1999). Their attractive and repulsive potential functions are formed using both exponential and power laws. The authors show (analytically and numerically) that repulsion terms must dominate attraction potentials at a short range for a well spaced biologically plausible group to form. Liapunov functions (Boyce & DiPrima 1992) are used to evaluate equilibrium positions resulting from their models.

Viscido et al. (2005) developed a three-dimensional simulation model based on attraction and repulsion interactive forces, to model fish movement. The authors examine the effects of the size of the population and

the number of interacting neighbours on the structure and mobility of the group. The forces in Viscido et al. (2005) are the sum of social and stochastic forces. Individual accelerations are calculated from these forces and used to update individual velocities. The repulsion and attraction forces are modelled as a linear step function. We shall use a sum of exponential forces for our cohesive force, as in Mogilner et al. (2003). We will show the desirability for a frictional force to prevent individuals escaping the confines of the group; Viscido et al. (2005) exclude the presence of friction in their model by assuming an upper limit to the magnitude of their individual forces. Viscido et al. (2005) quote a paper they have in preparation, where they discuss a force-based model, a variation is used in Viscido et al. (2005), utilising alignment and frictional forces.

We start with a model of cohesive forces, formulated as a physical force environment. We will introduce an alignment term designed to allow individuals to orient their velocities to one another. The forces in our model will act directly on velocities, unlike Mogilner et al. (2003) who allow their forces to act on the relative positions of each individual. Our approach allows the option of adopting existing physics knowledge and converting our Lagrangian system to an Eulerian approach (with Hamiltonian equations). We shall see that we will also have to introduce a dissipative force to the model, to prevent ‘escapees’ within the model. Further work could eliminate the need for this dissipative force.

5.2. Framework of the social potential model of collective behaviour

We formulate the social potential model of aggregative behaviour. We first consider cohesion forces (attraction and repulsion), before turning our attention to alignment forces in the model.

The forces in question act directly on individual velocities and not on their relative positions, as in Mogilner et al. (2003). We consider only pairwise interactions among individuals, we neglect higher order interactions on the basis that these are less likely to occur in comparison to the likelihood of pairwise interactions. We assume that individuals are subject to attractive, repulsive and alignment forces. However, unlike Chapters 3 and 4, these social forces are continuous in nature. The social forces acting on individuals in Chapter 3 are based on distinct nested spherical zones. In this section, the forces consist of overlapping continuous functions, the particular total force dictating the course of the individuals depends on inter-individual spacings.

Let the coordinates of the i -th individual ($i = 1, \dots, N$; where N is the number of individuals present in the system) in the group at time t be represented by the position vector $\mathbf{r}_i(t) = \mathbf{r}_i = (x_i, y_i, z_i; t)$ with an associated velocity of $\mathbf{v}_i(t) = \mathbf{v}_i$. Hence, $r_i^2 = |\mathbf{r}_i|^2 = x_i^2 + y_i^2 + z_i^2$. We assume that all the N individuals are identical.

We define the *social potential energy* associated with the i -th member at time t as $V(\mathbf{r}_i)$. The *social energy field* of the group at time t is $V(\mathbf{r}_1, \mathbf{r}_2, \dots, \mathbf{r}_N)$. Let \mathbf{r}_{ij} be the vector pointing from the i -th individual's position, to the j -th individual's location. Hence, $\mathbf{r}_{ij} = \mathbf{r}_j - \mathbf{r}_i = (x_{ij}, y_{ij}, z_{ij}; t)$, where $x_{ij} = x_j - x_i$ (likewise for y_{ij} and z_{ij}). For individual i at position \mathbf{r}_i , the total energy acting upon it at time t is

$$V_{total}(\mathbf{r}_i) = \sum_{j \neq i}^N V(\mathbf{r}_{ij}). \quad (5.1)$$

The sum extends over all other individuals in the model ($j = 1, \dots, N$; $j \neq i$).

Each individual seeks to move in a direction to minimise this social energy. The i -th individual's direction of travel at time t is therefore modified by a force $\mathbf{F}_{total}(\mathbf{r}_i) = -\nabla V_{total}(\mathbf{r}_i)$, at a rate $|\nabla V_{total}(\mathbf{r}_i)|$.

We need to select an appropriate form for our individual social energy function ($V(\mathbf{r}_i)$), which will be a sum of the contributing potentials. We assume radial symmetry in our potential functions.

Firstly, we consider the attraction and repulsion potential terms. Ideally, the attraction and repulsion potentials decay with increasing inter-individual distance. Consequently, individual i will have minimal interaction with distant individuals. A monotonically decreasing continuous function will fulfil this requirement. We follow Mogilner et al. (2003)'s lead and model the attractive and repulsive forces as decaying exponential functions:

$$\begin{aligned} V_{repulsion}(\mathbf{r}_i) &= \frac{A}{B}e^{-B(r_i+C)} \\ V_{attraction}(\mathbf{r}_i) &= -\frac{D}{E}e^{-E(r_i+C)} \\ V_{cohesion}(\mathbf{r}_i) &= V_{repulsion}(\mathbf{r}_i) + V_{attraction}(\mathbf{r}_i), \end{aligned} \quad (5.2)$$

where A , B , C , D and E are constants ($A, D \leq 0$ and $B, C, E \geq 0$). The units of A and D are $(\text{unit mass}) \times (\text{unit distance})^2 / (\text{unit time})^2$ and the units of C are unit distance, we shall assume these units without explicitly stating them. The A and D constants control the magnitudes of the repulsion and attraction potentials, respectively. The constants B and E govern the spread or range of the repulsion and attraction potentials. We call these two constants the repulsion and attraction ranges, respectively. The constant C allows us to further manipulate the potential functions and can be regarded as a body length. An example of $V_{cohesion}(\mathbf{r}_i)$ is shown in Figure 5.1. It is straightforward to derive an explicit expression for the social forces acting on individual i , due to these two social potentials

$$\begin{aligned} \mathbf{F}_{cohesion}(\mathbf{r}_i) &= \mathbf{F}_{repulsion}(\mathbf{r}_i) + \mathbf{F}_{attraction}(\mathbf{r}_i) \\ &= -\left(\frac{\partial V_{cohesion}}{\partial x_i}, \frac{\partial V_{cohesion}}{\partial y_i}, \frac{\partial V_{cohesion}}{\partial z_i} \right). \end{aligned} \quad (5.3)$$

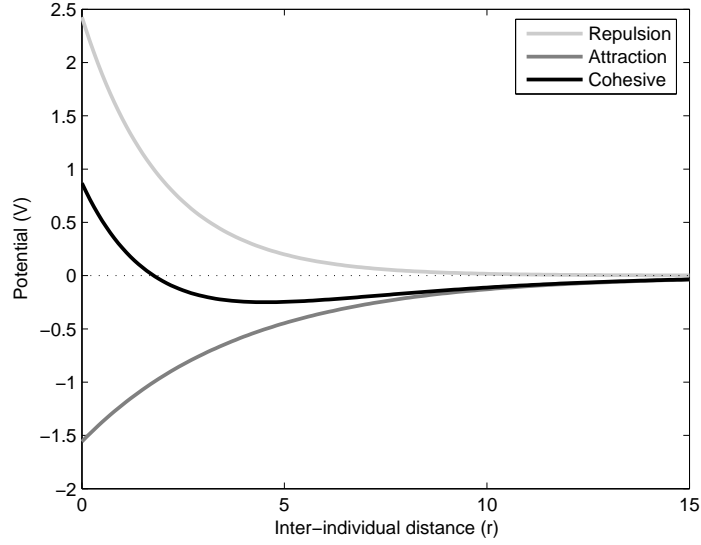


FIGURE 5.1. Example of the social cohesion potential function (Equation 5.2). Parameter values are $A = 2$, $B = 0.5$, $C = 0$, $D = 0.5$, $E = 0.1$.

Let the magnitude r_{ij} be written as $(r_{ij})^2 = (x_{ij})^2 + (y_{ij})^2 + (z_{ij})^2$, then $\frac{\partial r_{ij}}{\partial x_i} = x_{ij}/r_{ij}$. Now,

$$\frac{\partial V_{cohesion}}{\partial x_i} = \sum_{j \neq i}^N \frac{\partial V_{repulsion}(\mathbf{r}_{ij})}{\partial x_i} + \sum_{j \neq i}^N \frac{\partial V_{attraction}(\mathbf{r}_{ij})}{\partial x_i}. \quad (5.4)$$

Clearly,

$$\begin{aligned} \sum_{j \neq i}^N \frac{\partial V_{repulsion}(\mathbf{r}_{ij})}{\partial x_i} &= \frac{A}{B} \sum_{j \neq i}^N \frac{\partial}{\partial x_i} e^{-B(r_{ij}+C)} \\ &= -A \sum_{j \neq i}^N \frac{x_{ij}}{r_{ij}} e^{-B(r_{ij}+C)} \end{aligned} \quad (5.5)$$

and

$$\begin{aligned} \sum_{j \neq i}^N \frac{\partial V_{attraction}(\mathbf{r}_{ij})}{\partial x_i} &= -\frac{D}{E} \sum_{j \neq i}^N \frac{\partial}{\partial x_i} e^{-E(r_{ij}+C)} \\ &= D \sum_{j \neq i}^N \frac{x_{ij}}{r_{ij}} e^{-E(r_{ij}+C)}. \end{aligned} \quad (5.6)$$

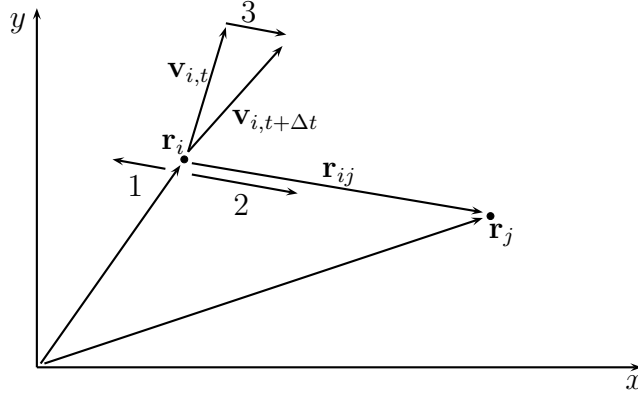


FIGURE 5.2. Simplified diagram of the attraction and repulsion forces acting on individual i , due to individual j . Vector 1 is $-\nabla V_{repulsion}$, 2 is $-\nabla V_{attraction}$, 3 is total force acting on individual i ($-\nabla V_{total}$).

Consequently,

$$-\frac{\partial V_{cohesion}}{\partial x_i} = \sum_{j \neq i}^N \frac{x_{ij}}{r_{ij}} (Ae^{-B(r_{ij}+C)} - De^{-E(r_{ij}+C)}). \quad (5.7)$$

Similar expressions can be derived for $-\frac{\partial V_{cohesion}}{\partial y_i}$ and $-\frac{\partial V_{cohesion}}{\partial z_i}$. We can derive an explicit solution to $\mathbf{F}_{cohesion}(\mathbf{r}_i)$

$$\mathbf{F}_{cohesion}(\mathbf{r}_i) = \sum_{j \neq i}^N (Ae^{-B(r_{ij}+C)} - De^{-E(r_{ij}+C)}) \hat{\mathbf{r}}_{ij}, \quad (5.8)$$

where $\hat{\mathbf{r}}_{ij}$ is the unit vector in the direction of the vector \mathbf{r}_{ij} . An example of this cohesion force is shown in Figure 5.2.

Social cohesion forces have been considered before (Mogilner et al. 2003, Viscido et al. 2005). We now consider a different perspective, by the addition of an alignment term to the potential model. This alignment term is designed to allow individuals to orient their velocities with one another.

We define the alignment potential of individual i at time t as

$$V_{alignment}(\mathbf{r}_i) = -F \frac{\mathbf{v}_i \cdot \mathbf{r}_i}{(r_i + C)^a} \quad (5.9)$$

where F and a are constants ($F, a \geq 0$). The units of F are (unit mass) \times (unit distance)²/(unit time)², we shall assume these units without explicitly stating them. The constant F controls the size of the alignment term, we call this constant the alignment magnitude. The alignment potential depends on a power law through the exponent a . Hence, the contribution from the j -th individual is minimal if the j -th individual is relatively distant from the i -th individual. The total alignment contribution to individual i at time t is $\sum_{j \neq i}^N V_{alignment}(\mathbf{r}_{ij})$. An example of the alignment force acting on individual i due to individual j , is illustrated in Figure 5.3.

The total alignment force acting on individual i at time t is calculated as:

$$\begin{aligned}
\mathbf{F}_{alignment}(\mathbf{r}_i) &= \frac{\partial}{\partial t} \left[\nabla_{\mathbf{v}_i} \left(\sum_{j \neq i}^N V_{alignment}(\mathbf{r}_{ij}) \right) \right] \\
&= \frac{\partial}{\partial t} \left[\nabla_{\mathbf{v}_i} \left(F \sum_{j \neq i}^N \frac{\mathbf{v}_{ij} \cdot \mathbf{r}_{ij}}{(r_{ij} + C)^a} \right) \right] \\
&= \frac{\partial}{\partial t} \left[F \sum_{j \neq i}^N \frac{\mathbf{r}_{ij}}{(r_{ij} + C)^a} \right] \\
&= F \sum_{j \neq i}^N \frac{\partial(\mathbf{r}_{ij} (r_{ij} + C)^{-a})}{\partial t}, \tag{5.10}
\end{aligned}$$

where $\nabla_{\mathbf{v}}$ is the direction differential operator with respect to the vector \mathbf{v} . In the calculation of (5.10) we have effectively used the chain rule, with \mathbf{r}_i , \mathbf{v}_i and t . Now,

$$\begin{aligned}
\frac{\partial}{\partial t} (\mathbf{r}_{ij} (r_{ij} + C)^{-a}) &= \frac{\partial}{\partial t} (\mathbf{r}_{ij}) (r_{ij} + C)^{-a} + \frac{\partial}{\partial t} ((r_{ij} + C)^{-a}) \mathbf{r}_{ij} \\
&= \mathbf{v}_{ij} (r_{ij} + C)^{-a} + \frac{\partial}{\partial t} ((r_{ij} + C)^{-a}) \mathbf{r}_{ij}. \tag{5.11}
\end{aligned}$$

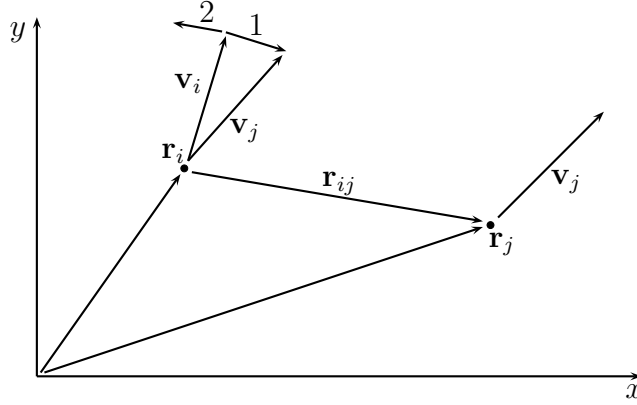


FIGURE 5.3. Simplified diagram of the alignment forces acting on individual i , due to individual j . Vector 1 is the first component of $-\nabla V_{alignment}$, 2 is the second component of $-\nabla V_{alignment}$.

We need to differentiate the term $(r_{ij} + C)^{-a}$ with respect to time:

$$\begin{aligned}
 \frac{\partial}{\partial t} ((r_{ij} + C)^{-a}) &= \frac{\partial}{\partial t} \left((x_{ij}^2 + y_{ij}^2 + z_{ij}^2 + C)^{-a/2} \right) \\
 &= -ar_{ij}^{-1} \left((x_{ij}^2 + y_{ij}^2 + z_{ij}^2)^{\frac{1}{2}} + C \right)^{-a-1} \\
 &\quad \times \left(x_{ij} \frac{dx_{ij}}{dt} + y_{ij} \frac{dy_{ij}}{dt} + z_{ij} \frac{dz_{ij}}{dt} \right) \\
 &= \frac{-a}{r_{ij} (r_{ij} + C)^{a+1}} \mathbf{v}_{ij} \cdot \mathbf{r}_{ij}. \tag{5.12}
 \end{aligned}$$

Consequently, (5.11) becomes:

$$\frac{\partial}{\partial t} (\mathbf{r}_{ij} (r_{ij} + C)^{-a}) = \frac{\mathbf{v}_{ij}}{(r_{ij} + C)^a} + \frac{-a (\mathbf{v}_{ij} \cdot \mathbf{r}_{ij}) \hat{\mathbf{r}}_{ij}}{(r_{ij} + C)^{a+1}} \tag{5.13}$$

and (5.10) becomes

$$\mathbf{F}_{alignment}(\mathbf{r}_i) = F \sum_{j \neq i}^N \left(\frac{\mathbf{v}_{ij}}{(r_{ij} + C)^a} - \frac{a (\mathbf{v}_{ij} \cdot \mathbf{r}_{ij}) \hat{\mathbf{r}}_{ij}}{(r_{ij} + C)^{a+1}} \right). \tag{5.14}$$

The first term in the summation in (5.14) is obviously a direct corrective term between \mathbf{v}_i and \mathbf{v}_j . The second term is more subtle. This term is similar to a cohesive force, in that it is parallel to the vector \mathbf{r}_{ij} . This dot product term acts on the i -th individual's velocity (\mathbf{v}_i), by changing \mathbf{v}_i so that it becomes aligned with \mathbf{v}_j . The direction of this second

term (either in the direction of \mathbf{r}_{ij} or $-\mathbf{r}_{ij}$) depends on the relative orientation of \mathbf{v}_i to \mathbf{v}_j . Once \mathbf{v}_i and \mathbf{v}_j are parallel, the alignment force contribution from individual j in (5.14) is zero.

The total force acting upon individual i at a particular time t is therefore

$$\begin{aligned} \mathbf{F}_{total}(\mathbf{r}_i) &= \mathbf{F}_{repulsion}(\mathbf{r}_i) + \mathbf{F}_{attraction}(\mathbf{r}_i) \\ &\quad + \mathbf{F}_{alignment}(\mathbf{r}_i) \\ &= \sum_{j \neq i}^N (Ae^{-B(r_{ij}+C)} - De^{-E(r_{ij}+C)}) \hat{\mathbf{r}}_{ij} \\ &\quad + F \sum_{j \neq i}^N \left(\frac{\mathbf{v}_{ij}}{(r_{ij}+C)^a} - \frac{a(\mathbf{v}_{ij} \cdot \mathbf{r}_{ij})}{(r_{ij}+C)^{a+2}} \mathbf{r}_{ij} \right). \end{aligned} \quad (5.15)$$

Thus far, the potential model is in a form amendable for a Hamiltonian formulation.

5.2.1. Selected mathematical relations of the potential model.

To generate biologically plausible behaviour in the potential model, we need to consider the relationships of the model parameters. We can use similar arguments to Mogilner et al. (2003) for the cohesion forces. Mogilner et al. (2003) show we need to have short range repulsion and long range attraction for biologically relevant behaviour.

Repulsive forces must be sufficiently strong to prevent the group collapsing into a dense cluster. This implies that repulsion must increase as inter-individual spacing decreases. Repulsion is therefore a short range force. At medium and longer ranges, attractive forces must dominate over repulsive forces. This requires $A \geq D$ and $B \geq E$.

We can define the ratios $\omega_1 = A/D$ and $\omega_2 = E/B$. Hence, we can rearrange the inequalities to give $\omega_1 \geq 1$ and $\omega_2 \leq 1$. There are no similar ratios to compare the alignment magnitude (F) with the attraction and repulsion forces. In general, it is difficult to obtain analytical results for the model with alignment forces.

It is useful to derive a *comfortable distance* ($\mathbf{r}^* = r^*\hat{\mathbf{r}}$), which occurs when repulsion and attraction terms are in equilibrium. This allows comparisons with Mogilner et al. (2003), who also derive this term.

The comfortable distance results from the equilibrium of the repulsion and attraction terms is given by

$$\begin{aligned} Ae^{-B(r+C)} &= De^{-E(r+C)} \\ \frac{A}{D} &= e^{(B-E)(r+C)} \\ \ln\left(\frac{A}{D}\right) &= (B-E)(r+C) \\ r+C &= \frac{\ln\left(\frac{A}{D}\right)}{B-E}. \end{aligned} \tag{5.16}$$

The comfortable distance magnitude (r^*) is

$$\begin{aligned} r^* &= \frac{\ln(\omega_1)}{B-E} - C \\ &= \frac{\ln(\omega_1)}{B(1-\omega_2)} - C. \end{aligned} \tag{5.17}$$

5.3. Results and discussion of model simulations

In this section, we will firstly show the need for a friction force. We shall consider the cohesive potential model (which is the potential model with repulsion, attraction and friction forces only) and the effect of the parameters on that model. We shall also consider the impact of the addition of an alignment term to the potential model. Finally, we shall compare the cohesion and alignment potential models. This section will commence with a justification of the use of dissipative forces in the potential model.

All simulations and figures in this chapter are generated in MATLAB (Version 7). The potential model requires only a matter of minutes to simulate, substantially faster than the models in Chapters 3 and 4.

5.3.1. The role of dissipative forces in the potential model.

We will have to introduce some kind of dissipative force into the potential model. With the current formulation (5.15), group members can escape the influence of the group and move off on their own accord if they have sufficient linear momentum, unaffected by any other individuals (we call these particular individuals ‘escapees’). This behaviour differs to the explosive behaviour seen in Chapter 3, which results from parameters chosen to cause repulsive behaviour. The escapees’ behaviour is due to excessive linear momentum. This is analogous to comets in planetary systems and is illustrated in Figure 5.4. This type of behaviour is biologically implausible, the biological group members should feel a desire to remain with the group. Viscido et al. (2005) avoid this problem by assuming an upper limit to the magnitudes of the forces in their model.

We introduce a dissipative force into the potential model, designed to prevent these escapees breaking away from the group. We model the dissipative force as a simple frictional force and allow it to directly act upon the individual velocities within the model. We define the dissipative force acting on individual i as

$$\begin{aligned}\mathbf{F}_{dissipate}(\mathbf{r}_i) &= -G|\mathbf{v}_i|^2\hat{\mathbf{v}}_i \\ &= -G|\mathbf{v}_i|\mathbf{v}_i,\end{aligned}\tag{5.18}$$

where $\hat{\mathbf{v}}_i$ is a unit vector and G is a positive constant, governing the rate of dissipation (the friction coefficient). We require negligible dissipation of energy at low velocities and dissipation to become more relevant as the size of the velocities increase. Hence, the quadratic dependence in the dissipative force term. This dissipative force term can be interpreted as an individual’s propensity to return to a resting state, a measure of an individual’s ‘laziness’. The dissipative force ($\mathbf{F}_{dissipate}(\mathbf{r}_i) = -G|\mathbf{v}_i|\mathbf{v}_i$) works directly against the combination of cohesive and alignment forces.

The total force acting upon individual i at a particular time t is therefore

$$\begin{aligned}
\mathbf{F}_{total}(\mathbf{r}_i) &= \mathbf{F}_{repulsion}(\mathbf{r}_i) + \mathbf{F}_{attraction}(\mathbf{r}_i) \\
&\quad + \mathbf{F}_{alignment}(\mathbf{r}_i) + \mathbf{F}_{dissipate}(\mathbf{r}_i) \\
&= \sum_{j \neq i}^N (Ae^{-B(r_{ij}+C)} - De^{-E(r_{ij}+C)}) \hat{\mathbf{r}}_{ij} \\
&\quad + F \sum_{j \neq i}^N \left(\frac{\mathbf{v}_{ij}}{(r_{ij} + C)^a} - \frac{a(\mathbf{v}_{ij} \cdot \mathbf{r}_{ij})}{(r_{ij} + C)^{a+1}} \hat{\mathbf{r}}_{ij} \right) \\
&\quad - G|\mathbf{v}_i|\mathbf{v}_i. \tag{5.19}
\end{aligned}$$

The consequences of the dissipative term are shown in Figure 5.5. The dissipative terms prevent escapees bolting and allow the individuals to settle in a stable cluster. We will further explore the impact of the friction coefficient (G) on the potential model and show that only a small amount of this friction force is required.

Just how much damping is required to prevent escapees? In order to answer this question, we simulate the cohesive model (no alignment terms) for various values of friction coefficient G . We use the model from Equation 5.20 with default parameters $A = 2$, $B = 0.5$, $C = 0$, $D = 1$ and $E = 0.25$ ($F = 0$).

Large expanses and average NND 's are (in this case) indicative of individuals 'overshooting' the group and becoming escapees. Figures 5.6 and 5.7 show a dramatic decrease in expanse and average NND 's once G is of the order of 10^{-3} and above. After the transition point of 10^{-3} , expanses and average NND 's stabilise, due to a cluster forming. We conclude for the cohesive potential model, that G should be at least as large as 10^{-3} to prevent breaks occurring. We will now consider how the friction coefficient affects the full model with an alignment term.

To evaluate the influence of the dissipative forces in the alignment model, we use the model from (5.19) with default parameters $A =$

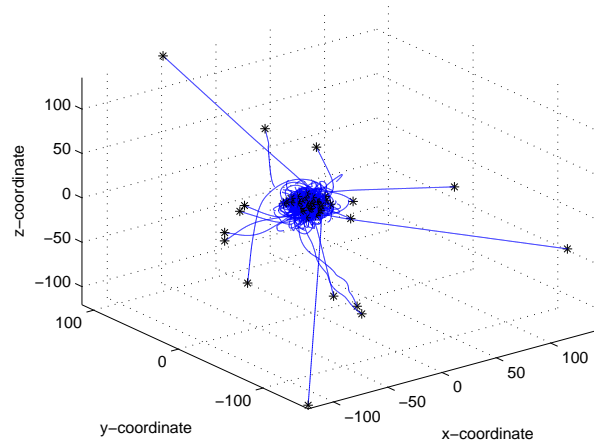


FIGURE 5.4. Simulation of the potential model, with cohesive terms only ($A = 2$, $B = 0.5$, $C = 0$, $D = 1$, $E = 0.25$, $F = 0$, $N = 50$). There are no dissipative forces present. Blue lines indicate trajectories during the simulation and black points indicate final positions of individuals.

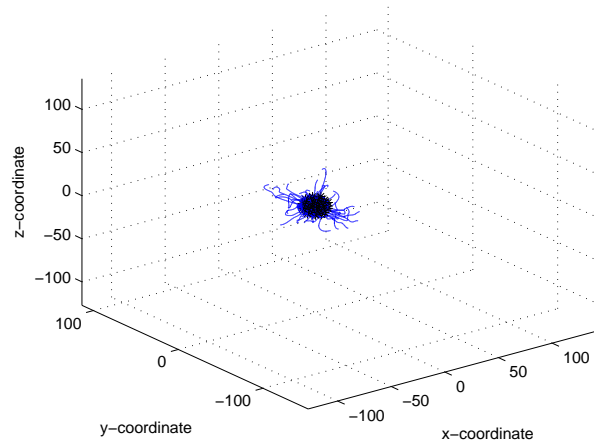


FIGURE 5.5. The simulation in Figure 5.4, with a dissipative term ($G = 0.01$). This dissipative force arrests excessive centripetal motion, the group forms a stable group.

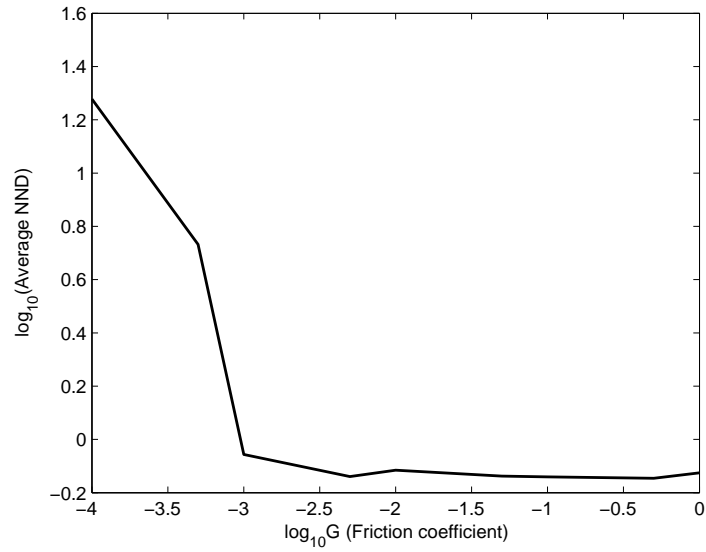


FIGURE 5.6. Effect of G (friction coefficient) on the average nearest-neighbour distance of the group. Scales of both axes are logarithmic.

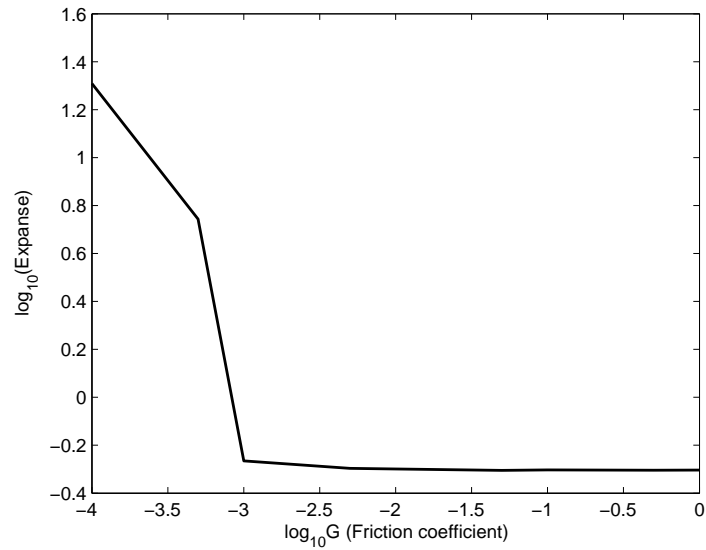


FIGURE 5.7. Effect of G (friction coefficient) on the expansion of the group. Scales of both axes are logarithmic.

2, $B = 0.5$, $C = 0$, $D = 1$, $E = 0.25$ and $F = 0.2$. We use the statistics of gross distance (the actual distance individuals travel in the simulation, see (2.9)) and the magnitude of the velocities (speed) of the individuals at the end of the simulation. We take average values of these statistics over the entire group. We include error bounds, which are derived from the standard deviation of the distribution of the sample mean multiplied by the appropriate t -value. These error bounds are negligible in other figures, hence we have neglected these errors. Clearly, the greater the friction force acting on individuals, the slower the individuals will travel. This should manifest as smaller speeds. If individuals are travelling at lower speeds, they will cover less distance in the model, hence gross distance will be reduced with increased values of G .

In general, reduced gross distances and speeds result from an increased level of frictional force. This is apparent in Figure 5.8. We include Figure 5.9, which demonstrates that frictional force has minimal impact on polarisations and momenta. Logically, the frictional force only acts to slow individuals. It has no bearing in an individual's inclination to align with its neighbours. Hence, dissipative force will have little effect on group polarisation.

The Hamiltonian description requires gradient forces, a friction force is not a gradient force. By introducing friction to the model, we lose the opportunity to use a Hamiltonian description of this system. However, we have shown we only need a small amount of friction, which will enable us to carry out our analysis and see numerically and simulation-wise how a Hamiltonian formulation should behave. Further work to gain an Eulerian description could be to include an additional attraction gradient force that acts on individuals at longer distances than the current repulsion and attraction forces. This attraction force

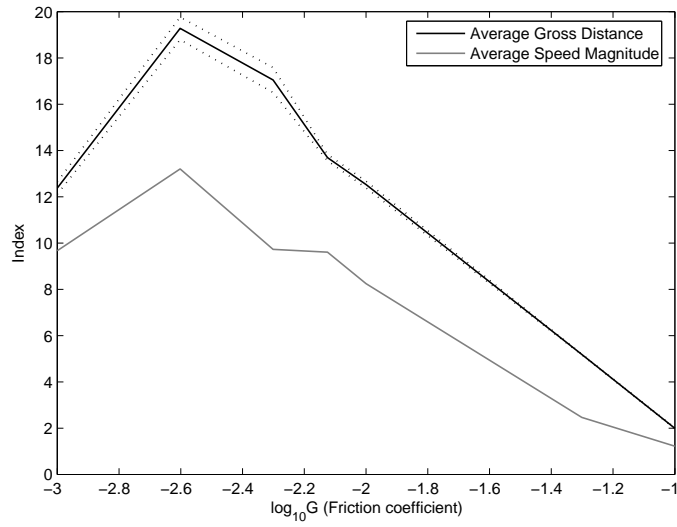


FIGURE 5.8. Effect of the friction coefficient (G) on the alignment model. Dashed lines indicate error bounds. The average speed magnitudes are multiplied by a factor of 10, for comparative purposes. Other parameters as in Figure 5.24.

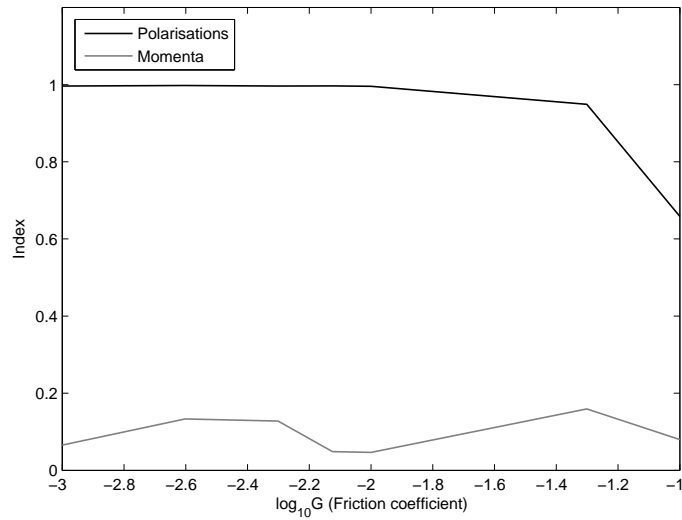


FIGURE 5.9. Effect of the friction coefficient (G) on group polarisations and momenta. Other parameters as in Figure 5.24.

should be an attraction to the group as a whole, rather than to individuals. Escapees experience a desire to rejoin the group once they are beyond the influences of the current attraction force.

5.3.2. Simulation of the cohesive potential model. We turn our attention to the cohesive model, with attraction, repulsion and dissipative terms, but no alignment terms ($F = 0$), namely

$$\begin{aligned} \mathbf{F}_{total}(\mathbf{r}_i) &= \mathbf{F}_{repulsion}(\mathbf{r}_i) + \mathbf{F}_{attraction}(\mathbf{r}_i) + \mathbf{F}_{dissipate}(\mathbf{r}_i) \\ &= \sum_{j \neq i}^N (Ae^{-B(r_{ij}+C)} - De^{-E(r_{ij}+C)}) \hat{\mathbf{r}}_{ij} \\ &\quad - G|\mathbf{v}_i|\mathbf{v}_i. \end{aligned} \tag{5.20}$$

We shall compare this model with results from Mogilner et al. (2003) and gain insights into the interaction of the parameters.

We use the model from Equation 5.20 with default parameters $A = 2$, $B = 0.5$, $C = 0$, $D = 1$, $E = 0.25$ and $G = 0.01$, unless stated otherwise. We run our simulations for 50 individuals ($N = 50$), each starting from random positions and we allow the simulations to run for 1000 timesteps. Unless discussed otherwise, this will be our baseline model in this section.

Since we are examining a repulsion and attraction model, there is no incentive for individuals to align their velocities with one another. The cohesive forces affect the ‘closeness’ of the group members. Hence, nearest-neighbour distance (NND , 2.7) and expanse (2.8) will be the most useful descriptive statistics in analysing the outcomes of the simulations. Expanse measures the overall size of the group, while NND measures inter-individual distances. The average NND for the group reflects the average density of individuals. An increasing NND implies that the inter-individual distances are increasing and the group members are becoming more and more spread apart, that is, the density of the group is decreasing.

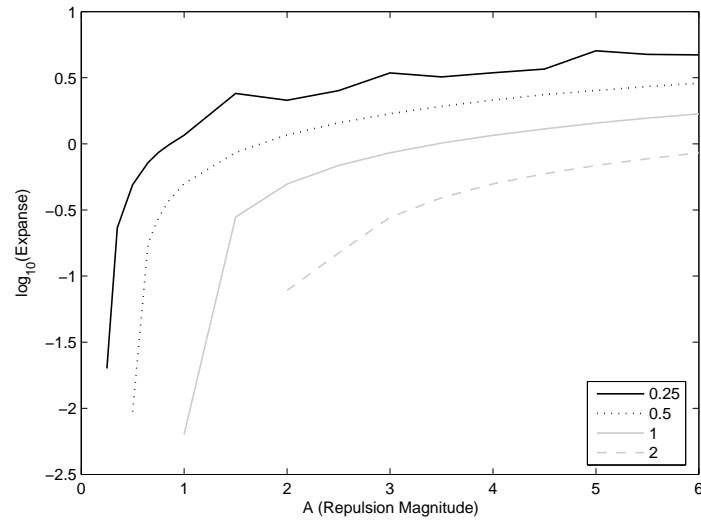


FIGURE 5.10. Effect of A on the expanse of the group from the cohesive potential model. Different values of D are considered (indicated by the legend).

The parameters A and D govern the relative sizes of the repulsion and attraction forces, respectively. Logically, as A increases (or, relative to D , the ratio ω_1 increases) the repulsive force becomes dominant over the attraction force. As this occurs, individuals will experience larger repulsion forces, causing the group to expand and become more diffused. Conversely, increasing D (relative to A) results in stronger attraction forces, causing individuals to form a denser, more compact group.

In order to produce a smaller denser group, we expect that we shall have to reduce A and increase D , relative to one another. A compact group should result as the ratio ω_1 tends towards 1 (recall $A \geq D$ for biologically relevant behaviour in the potential model).

The interactions between the repulsion and attraction magnitudes are illustrated in Figures 5.10 to 5.14. Figures 5.10 and 5.11 show the consequences of increasing the repulsion magnitude (A), while holding the other parameters of the model constant (illustrated for different

values of the attraction magnitude, D). As A increases, group expanses and average NND 's tend to increase. Hence, with increasing repulsive forces, the group members are forced apart and the group becomes less dense (as predicted).

We can see the practicalities of these observations in Figures 5.11 and 5.10. Both figures show a tendency for expanse to increase and average density to decrease, as A increases relative to D . Conversely as the attraction magnitude (D) increases, the attraction forces become larger and the individuals in the group become closer to one another. This is shown in Figures 5.12 and 5.13, which consequently have decreasing average NND 's and group expanses, as D increases.

The consequence of an increasing repulsion range (B) parameter is shown in Figures 5.15 and 5.16. As B increases, the repulsion force diminishes exponentially and this is reflected in the decreasing expanses and average NND 's in Figures 5.15 and 5.16. The individuals are tending to settle in denser and denser clusters as B increases. Likewise, as the attraction range (E) increases, the attraction forces deteriorate exponentially. Repulsion forces dictate the behaviour of individuals and this is revealed in Figures 5.17 and 5.18, where expanse and average NND are increasing as E increases. In general, individuals in the group are tending to avoid one another (due to relatively low attraction forces) and an unstructured diffuse group forms.

Figure 5.14 shows the impact of changes in the combination of the two parameters A and D . A compact cluster results from reducing A and increasing D (decreasing the ratio ω_1). Group expanses and average NND 's decrease with decreasing ω_1 . The corresponding comfortable distances (r^*) has been included in Figure 5.14. Mogilner et al. (2003) observed that inter-individual distances in large groups will always be smaller than the equilibrium distance (r^*) between two individuals (distinct from a group) in their model. Our findings bear this

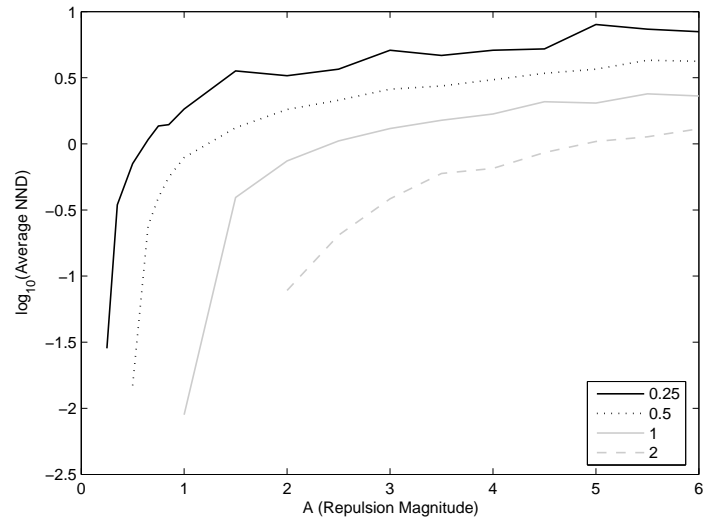


FIGURE 5.11. Effect of A on the average nearest-neighbour distance of the group from the cohesive model. Different values of D are considered (indicated by the legend).

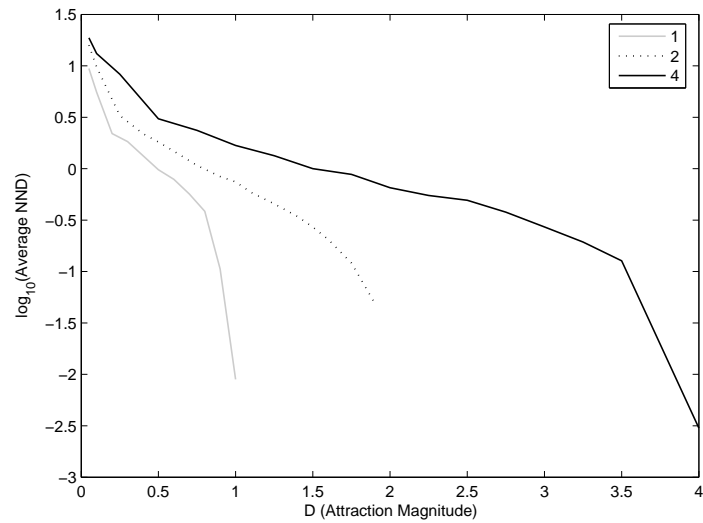


FIGURE 5.12. Effect of D on the average nearest-neighbour distance of the group. Different values of A are considered (indicated by the legend).

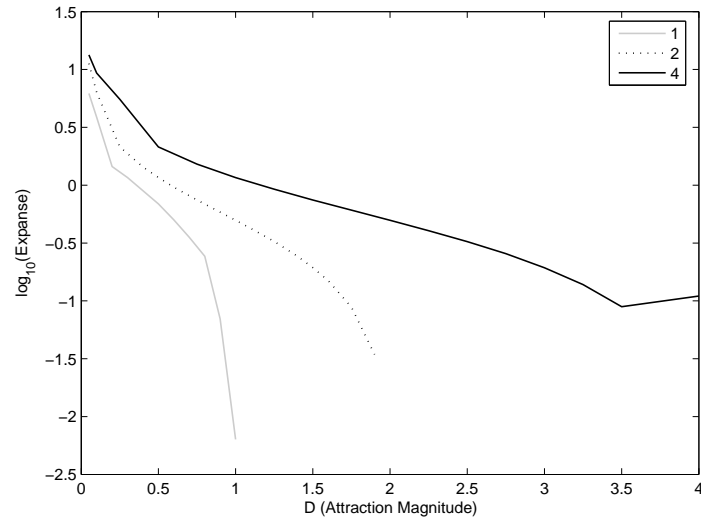


FIGURE 5.13. Effect of D on the expanse of the group. Different values of A are considered (indicated by the legend).

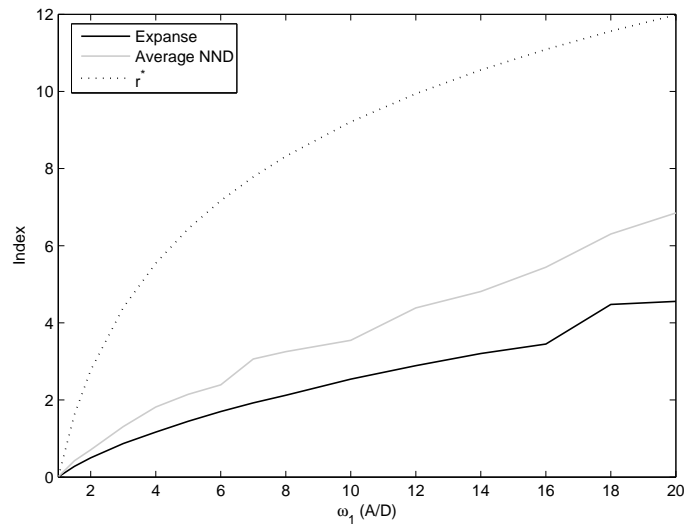


FIGURE 5.14. Expanse and average NND as a function of the ratio $\omega_1 (A/D)$. Comfortable distance (r^*) is also drawn, for comparison with average NND .

out, the *NND*'s from the group are consistently smaller than the corresponding comfortable distances (taking into account standard errors).

We turn our attention to the repulsion and attraction ranges, B and E (respectively) and see how these parameters affect the potential model. These parameters are involved in the decaying exponential terms in the repulsion and attraction potentials. Hence, B and E govern the spatial range of the repulsion and attraction forces. The smaller these two parameters are, the slower the rate of decay of the forces and the larger the spatial extent (or 'reach') of the forces. As the repulsion range (B) increases, the repulsion term decays more rapidly and individuals in the group effectively have less repulsive interactions with other individuals. With diminished repulsion forces, the group is expected to settle into a dense cluster. Similarly, as the attraction range (E) increases, the exponential term in the attraction force decays more rapidly and there is effectively less attraction, so that repulsive forces dictate the behaviour of the individuals. With minimal attraction forces present, individuals tend to avoid one another and an unstructured group results.

To create a dense compact group, we expect that we shall have to decrease E and increase B , relative to one another. The ratio $\omega_2 = E/B$ is bounded above by 1 ($B \geq E$) for biologically relevant behaviour. We expect that as ω_2 decreases to 1, a compact group will result.

If we want to produce an organised, clustered group, we can see from Figures 5.15 to 5.18 that increasing B and decreasing E will cause this. Effectively we are reducing the repulsion range, while increasing the attraction. Hence, the ratio ω_2 (E/B) is decreasing. Figure 5.19 shows the effects of this, where expanse and average *NND* decrease with decreasing ω_2 resulting in a compact group.

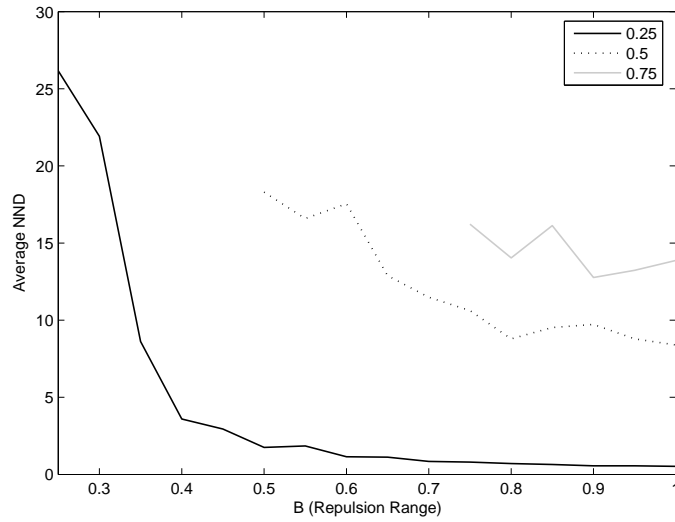


FIGURE 5.15. Effect of B on the average nearest-neighbour distance of the group. Different values of E are considered (indicated by the legend).

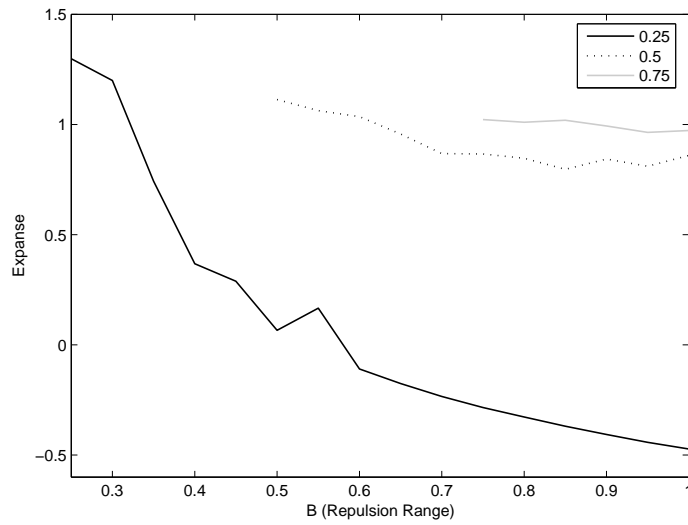


FIGURE 5.16. Effect of B on the expanse of the group. Different values of E are considered (indicated by the legend).

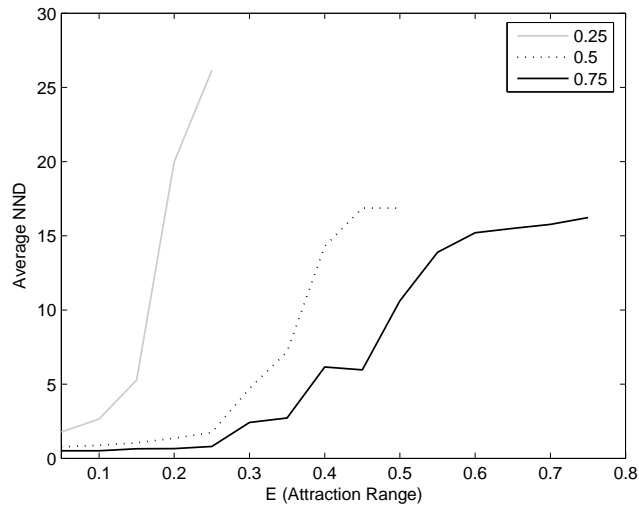


FIGURE 5.17. Effect of E on the average nearest-neighbour distance of the group. Different values of B are considered (indicated by the legend).

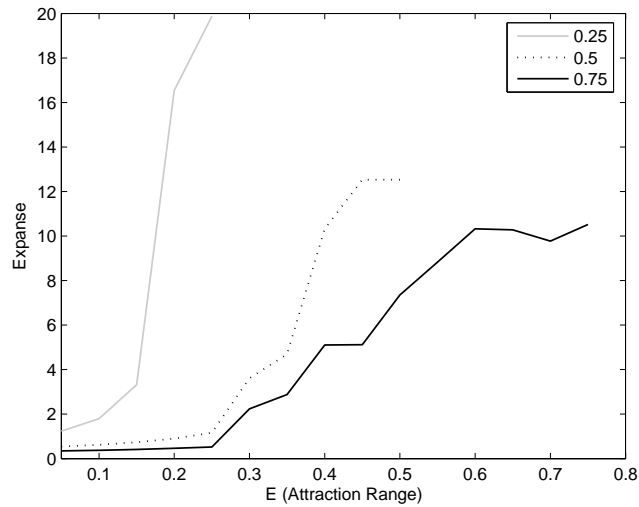


FIGURE 5.18. Effect of E on the expanse of the group. Different values of B are considered (indicated by the legend).

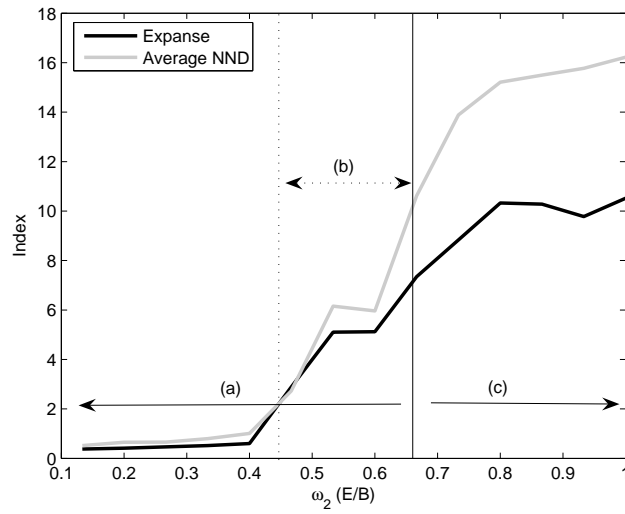


FIGURE 5.19. Expanses and average *NND* as a function of the ratio $\omega_2 (E/B)$. Transition zones marked by vertical lines ((a) single group, Figure 5.20; (b) separate distinct groups, Figure 5.22; (c) no organised group, Figure 5.21).

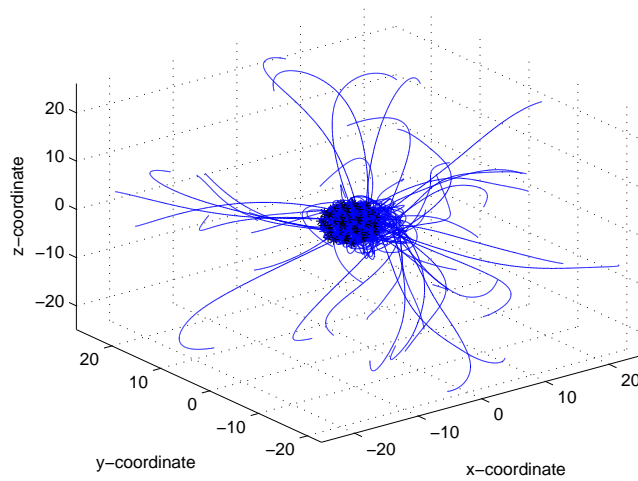


FIGURE 5.20. An example of clustered, dense group behaviour resulting from lower attraction range.

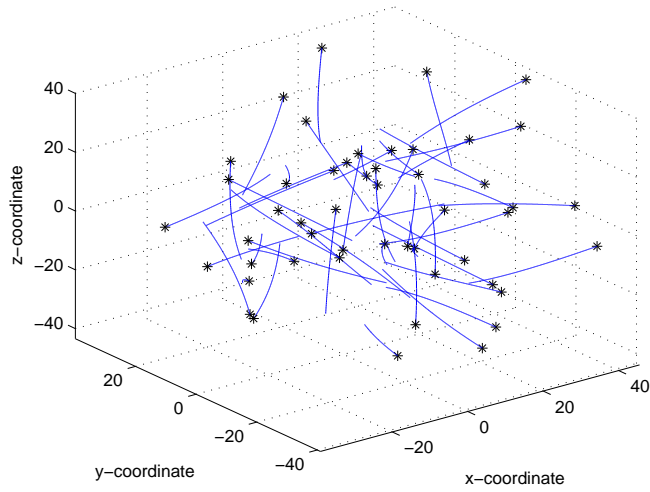


FIGURE 5.21. An example of swarm group behaviour resulting from the cohesive model. Repulsion forces dominate over attraction forces, so that individuals are prevented from coalescing.

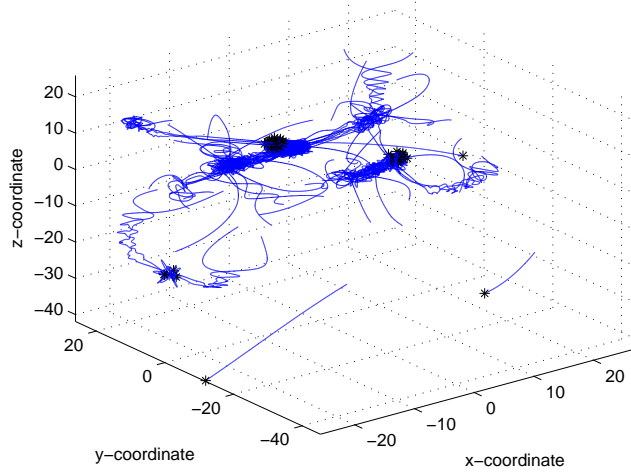


FIGURE 5.22. An example of separate, distinct groups forming with medium attraction ranges. Attraction forces can hold several individuals together, but not an entire group.

However, there is interesting behaviour in the model occurring behind the scenes, that Figures 5.17 and 5.18 do not reveal. Transitory behaviour occurs where individuals form an unorganised dispersed group, to move to several distinct small clusters of individuals and finally culminating in a single approximately spherical-shaped group. Mogilner et al. (2003) also noted a tendency for individuals to form groups that are nearly round (where the diameter of the group is dependent on the square root of the number of individuals), given the appropriate parameters. These transitions are marked on Figure 5.19. At small values of E (relative to B) individuals form a single group (approximately $E \leq 0.3$ or $\omega_2 \approx 2/3$, marked as (a) on Figure 5.19). This is shown in Figure 5.20. Above this boundary ($\omega_2 \rightarrow 1$, marked as (c) in Figure 5.19), these attraction forces are no longer strong enough to hold individuals together and the members deteriorate into an unorganised group (Figure 5.21). There may be a transitional behaviour between the two extremes, where individuals form into separate distinct clusters because attraction forces are not strong enough to cause individuals to bind together in a single group (roughly, $2/3 \leq \omega_2 \leq 10/11$, marked as (b) in Figure 5.19 and shown in Figure 5.22). This tends to happen with relatively larger values of B , where there are minimal repulsion forces. Attraction forces dominate the behaviour of the individuals, yet are too small in themselves to allow the individuals to form one single group. In fact, the cluster (Figure 5.20) is a stable state, while swarming behaviour (Figure 5.21) is inherently unstable. The distinct group (Figure 5.22) is quasi-stationary, meaning the smaller groups coalesce into larger groups, as can be seen in the trajectories in Figure 5.22.

5.3.3. Simulation of the alignment potential model. We consider the full model (5.19) with an alignment force. We use the model from (5.19) with default parameters $A = 2$, $B = 0.5$, $C = 0$, $D = 1$,

$E = .25$, $F = 0.2$, $a = 1$ and $G = 0.01$. We run our simulations for 50 individuals ($N = 50$), starting from random positions and we allow the simulations to run for 1000 timesteps. Unless discussed otherwise, this will be our reference model for this section.

Given that individuals under the influence of the alignment force will move together in a polarised arrangement, what role do the alignment and repulsion (cohesion forces) play in the model? We expect from discussions in Section 5.3.2 that stronger cohesion forces will cause a cluster, which will have individual velocities aligned. Figures 5.23 and 5.24 show the practical consequences behind increased cohesion forces. While the individuals in Figure 5.23 travel in a polarised group, relatively weak cohesion forces are present. The alignment terms cause the group to travel as an entity, but the shorter range attraction and repulsion forces result in the individuals forming separate clusters. Each cluster member's trajectories oscillate around one another (as is seen in Figure 5.23), due to the short range cohesive forces in the model. The cohesive forces are not strong enough to cause the members in the group to attract to all the other individuals, and therefore the group doesn't form a stable ovoid shape. The alignment forces are strong enough to cause the whole group to travel. With stronger cohesion forces, we can see the individuals first sorting themselves in Figure 5.24 due to the stronger cohesion forces, before alignment forces take control and the group travels as a coherent compact cluster. Figure 5.25 shows the relationship between the relative size of the cohesion forces and the size and density of the group. As cohesion forces decrease, the group becomes larger in size and inter-individual spacing increases, as predicted.

There are two parameters involved in the alignment force, the alignment magnitude (F) and the exponent in the power law (a). Clearly, F controls the overall size of the alignment force and a affects the radial extent of the reach of the alignment force.

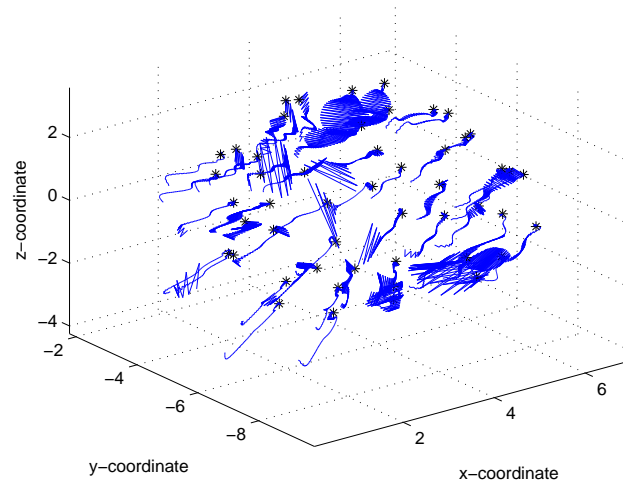


FIGURE 5.23. Example of a coherent group from the alignment potential model, resulting from relatively weak cohesion forces ($A = 0.2$, $B = 0.5$, $C = 0$, $D = 0.05$, $E = .25$, $F = 0.2$, $G = 0.01$).

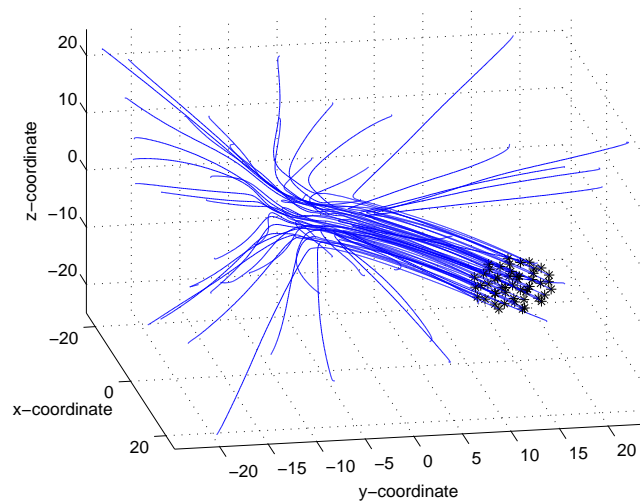


FIGURE 5.24. Example of a coherent group resulting from stronger cohesion forces than those in Figure 5.23 ($A = 2$, $B = 0.5$, $C = 0$, $D = 1$, $E = .25$, $F = 0.2$, $G = 0.01$).

Generally speaking, we expect that as the value of F increases, there will be an increased alignment effect present. This will give the individuals within the group greater incentive to align, which should be manifested particularly in the group polarisations.

This is illustrated in Figure 5.26, where we have altered the alignment magnitude (whilst holding the other parameters constant). As F increases in size, polarisation increases. The alignment magnitude has little effect on momentum (as expected). Practically speaking, it appears that only small alignment forces are required to result in a coherently directed group.

As seen in Figure 5.26, a transition in polarisations occurs at values of F in the region of 0.15 to 0.2. Before this region, the alignment magnitude is reduced relative to the attraction and repulsion forces. The individuals tend to form a compact cluster, due to these increased forces. This is shown by the decreased expanses and average NND 's in Figure 5.27. As the alignment magnitude increases, inter-individual spacing and group size increase.

As discussed in Section 5.3.2, the main effect on the model due to the cohesion forces is caused by the attraction and repulsion ranges (B and E), as these terms are involved in the exponential decays. The parameters B and E are also involved in the constant terms multiplying the exponential terms, but these are negligible in comparison to the effect of the exponential terms.

We mentioned in Section 5.3.2 that the effects of increasing the attraction and repulsion ranges are to decrease and increase the size of the group, respectively. We expect the same effect in the model with the alignment terms, as the cohesion forces have no bearing on the polarisations of the group.

Figures 5.28 and 5.29 show the impact of parameter B on the expanse and average density of the group. As the repulsion range increases, attraction forces dominate and the group becomes a compact

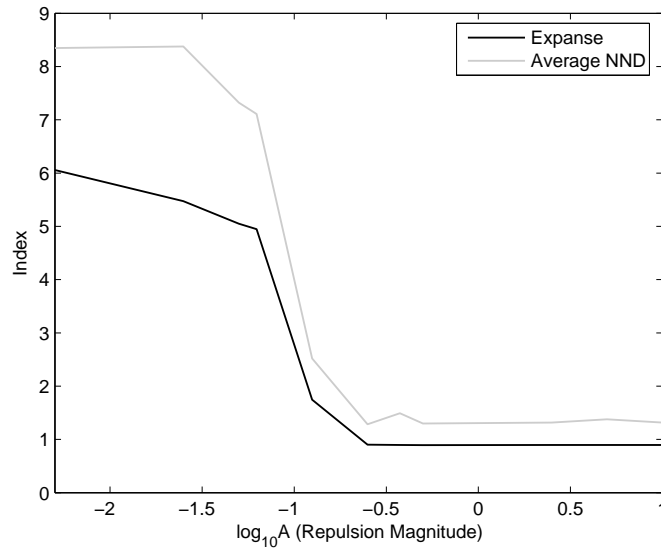


FIGURE 5.25. Effect of increased cohesion forces on the size of the group from the alignment model. The ratio ω_1 is preserved at 4 ($B = 0.5$, $C = 1$, $E = 0.25$, $F = 0.2$, $G = 0.01$).

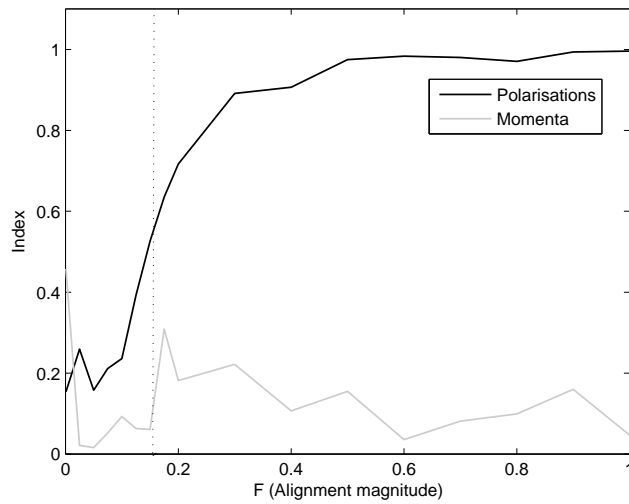


FIGURE 5.26. Effect of alignment magnitude (F) on group polarisations and momenta (other parameters as in Figure 5.24). The dashed lines indicate the emergence of an aligned group formation.

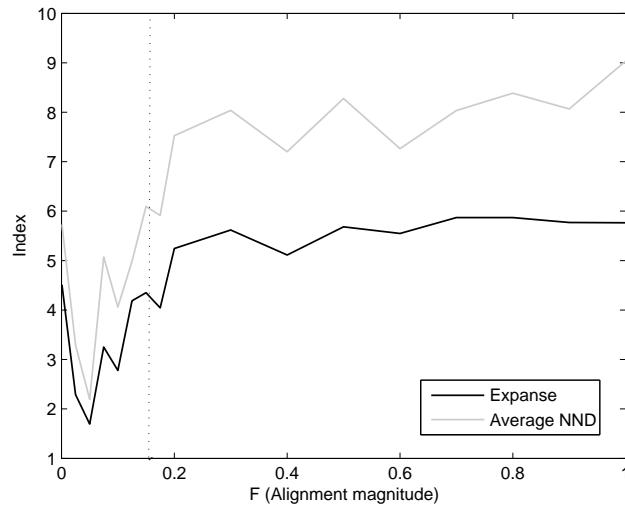


FIGURE 5.27. Effect of alignment magnitude (F) on group expanse and average NND (other parameters as in Figure 5.24).

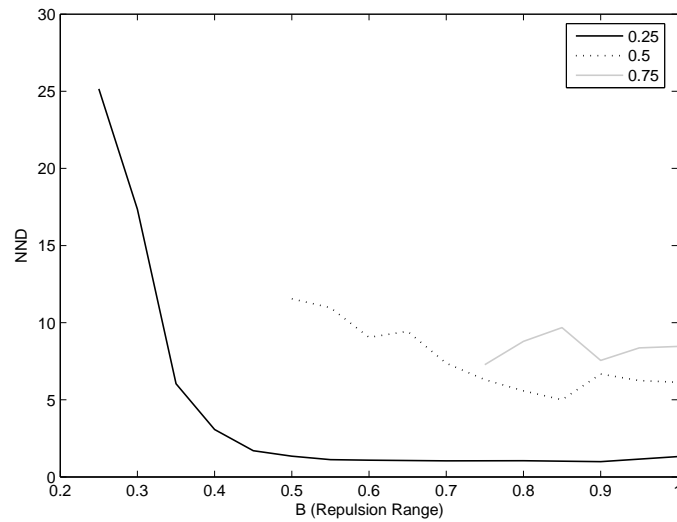


FIGURE 5.28. Effect of increased repulsion range (B) on the size of the group in the alignment model (other parameters as in Figure 5.24). Different values of E are considered (indicated by the legend).

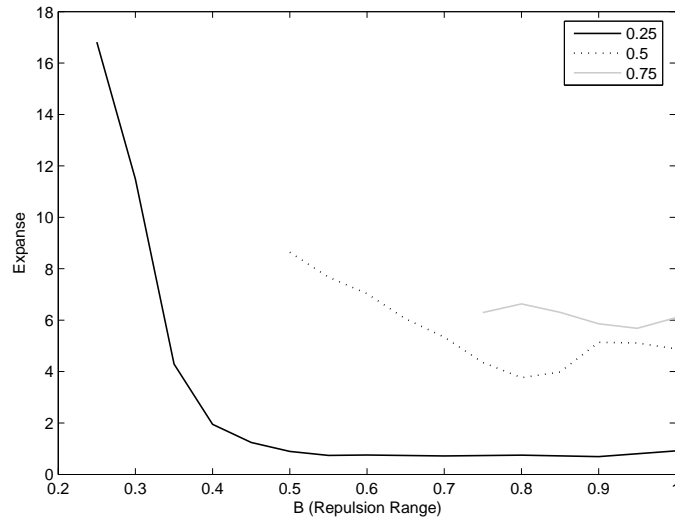


FIGURE 5.29. Effect of increased repulsion range (B) on the size of the group in the alignment model (other parameters as in Figure 5.24). Different values of E are considered (indicated by the legend).

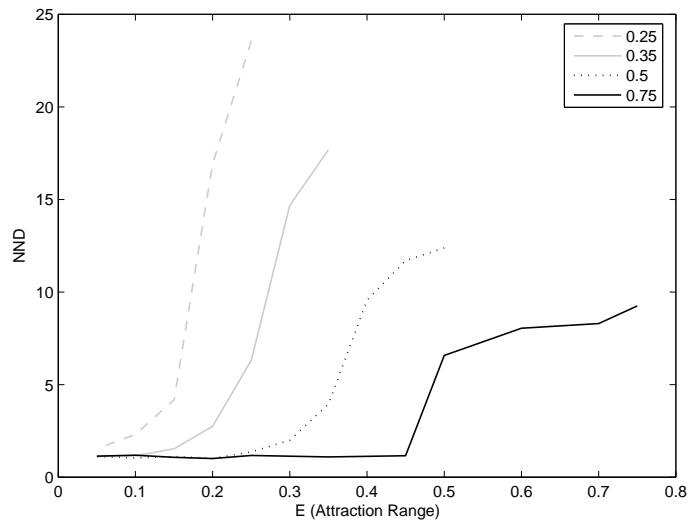


FIGURE 5.30. Effect of increased attraction range (E) on the size of the group in the alignment model (other parameters as in Figure 5.24). Different values of B are considered (indicated by the legend).

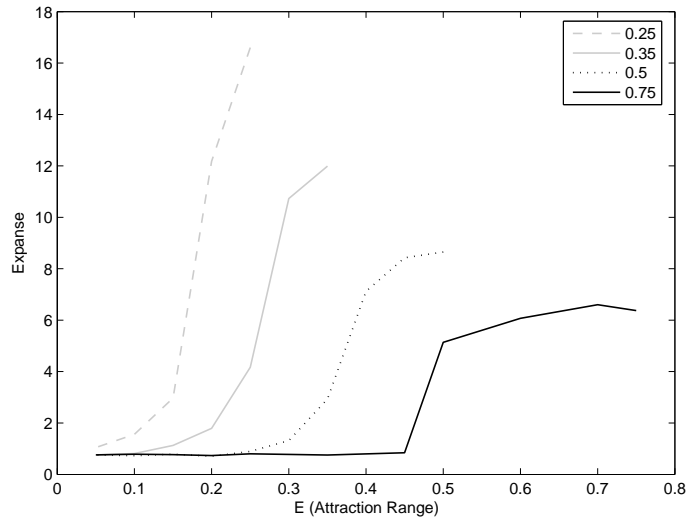


FIGURE 5.31. Effect of increased attraction range (E) on the size of the group in the alignment model (other parameters as in Figure 5.24). Different values of B are considered (indicated by the legend).

cluster. This is reflected in the decreasing group expanses and average NND 's, as B increases. Conversely, as E increases, attraction forces become negligible and the behaviour of the group is controlled by repulsion forces. Consequently, as shown in Figures 5.30 and 5.31, an increased E parameter results in a diffuse group with large group expanses and average NND 's.

As the magnitude ratio ω_1 increases, so does the polarisation (Figure 5.32). The group is tending to maintain an organised configuration, due to more attractive forces and relatively less repulsive ones. Effectively, for values of $\omega_1 \geq 4$, the group has evolved from a swarm to a polarised group.

If the range ratio ω_2 increases, this is due to either the parameter E increasing, and/or the parameter B decreasing. Either way, as ω_2 increases, there will be less attraction and relatively more repulsion

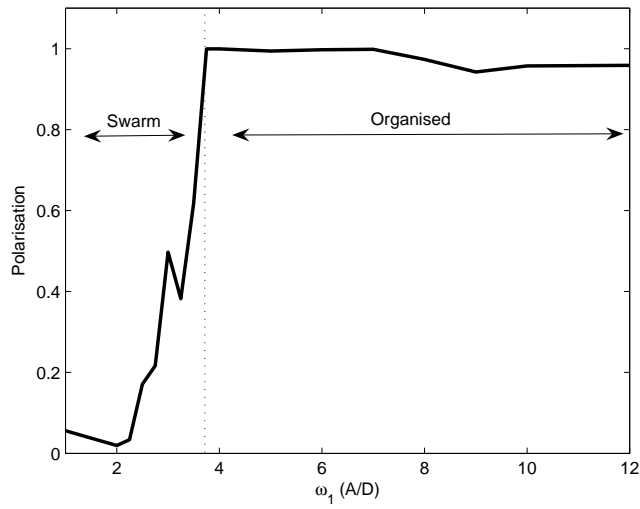


FIGURE 5.32. Polarisation as a function of the magnitude ratio ω_1 (A/D). Other parameters as in Figure 5.24.

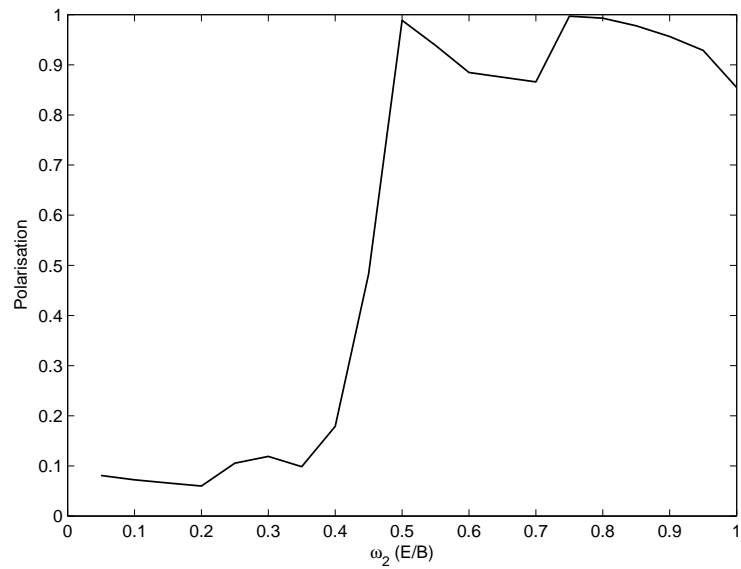


FIGURE 5.33. Polarisation and alignment force proportion as a function of the range ratio ω_2 (E/B). Other parameters as in Figure 5.24.

present in the system. Consequently, a more dispersed group should result. This has been discussed in Section 5.3.2.

As shown in Figure 5.33, with ω_2 increasing, so does the polarisation of the group. We can see from Figure 5.19 that as ω_2 increases, swarm behaviour results. We have the attraction forces balancing with the repulsion forces (as $E \rightarrow B$). This allows the alignment forces to become the dominant forces in the model, resulting in polarised groups.

For values of ω_2 in the range of 0 to approximately 0.5, swarms form, where the attraction and repulsion forces dominate. Beyond this region, alignment forces dominate and a coherent group results.

5.3.4. Comparison of cohesion and alignment models. We compare the potential model consisting purely of cohesive forces (Section 5.3.2) and the model with alignment forces (Section 5.3.3), referred to as the cohesion model and alignment model, respectively. We will show that alignment forces are crucial for individuals to travel as a group. Cohesive forces alone do not provide enough impetus.

Figures 5.34 and 5.35 show precisely what we mean by the previous statement. These figures show the last movements of the individuals in a cohesive model (corresponding to Figure 5.20) and an alignment model (Figure 5.24). Individuals in both models form stable ovoid clusters. However, the individuals in Figure 5.35 collapse into a cluster that as an entity does not travel. Conversely, the members of the group in Figure 5.34 form a stable cluster and advance as an entirety. Interestingly, the speeds of individuals in both models are of similar magnitudes. In fact, the individuals in the aligned group move comparatively slightly more slowly than the cohesive group (Figure 5.36). If the individuals in the latter model are moving faster, they must be moving around a centre and not travelling as a group. We shall show this by using polarisations and net to gross displacement ratio

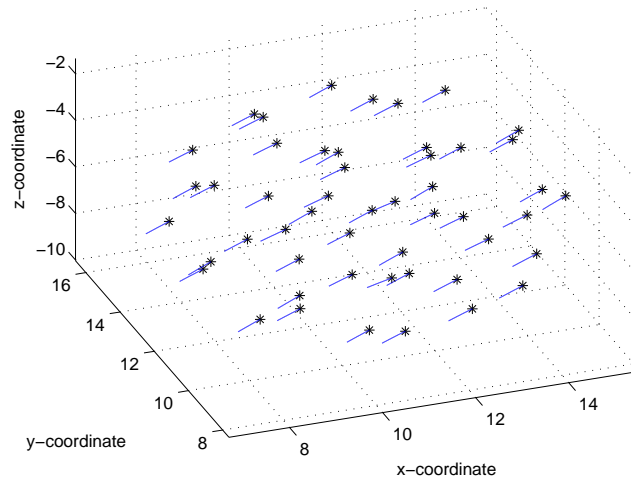


FIGURE 5.34. Final movements of the group with alignment forces (corresponding to Figure 5.24). Parameter values are $A = 2$, $B = 0.5$, $C = 0$, $D = 0.5$, $E = 0.25$, $F = 0.2$, $G = 0.01$.

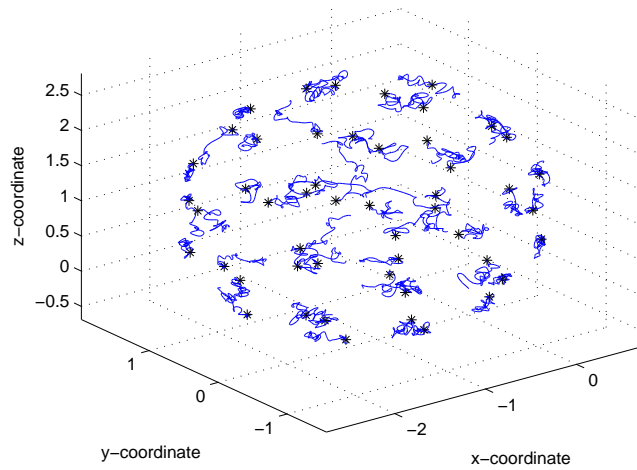


FIGURE 5.35. Final movements of the group without alignment forces (corresponding to Figure 5.20). Parameter values are $A = 2$, $B = 0.5$, $C = 0$, $D = 0.5$, $E = 0.1$, $G = 0.01$.

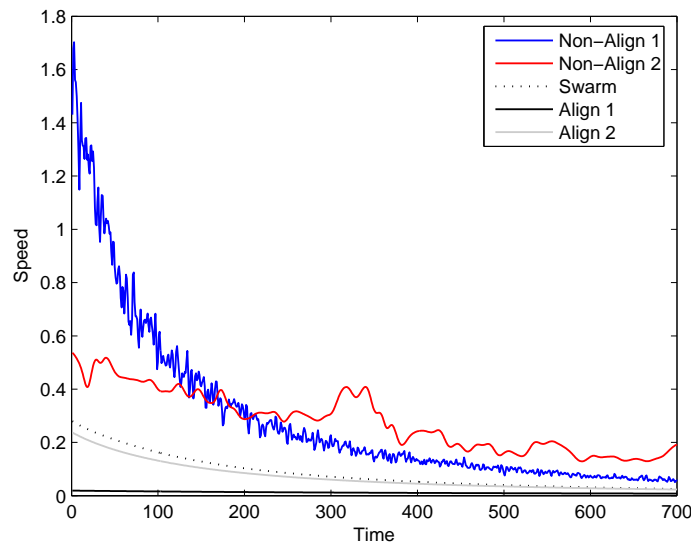


FIGURE 5.36. Average speed (velocity magnitude) of individuals in models, during the period of the simulations. The labels ‘Non Align 1’ refers to the model from Figure 5.20, ‘Non Align 2’ to Figure 5.22, ‘Swarm’ to Figure 5.21, ‘Align 1’ to Figure 5.23 and ‘Align 2’ to Figure 5.24.

(*NGDR*, 2.9). Recall that polarisation measures the degree of alignment amongst individuals, while *NGDR* measures the linearity of the path taken by each individual in the group. It is the group (not the group members) which travels faster in the alignment model, compared to the sedentary group in the cohesive model. We shall show this using *NGDR*’s.

We calculate *NGDR*’s for individuals in five models, those represented in Figures 5.20, 5.21, 5.22, 5.23 and 5.24. The first three figures refer to cohesive models (resulting in a single cluster, several distinct clusters and swarm formations as equilibrium positions, respectively) and the last two alignment models (where the individuals have either weak or stronger cohesive forces, respectively). We allow the individuals time to organise themselves, before calculating the *NGDR* values

(from 150 timesteps). Figure 5.24 clearly shows attractive and repulsive forces dominate the behaviour of the individuals initially, before alignment forces come into play. We ignore this initial sorting period. Figure 5.37 shows boxplots of the results.

Two cohesive models stand out as having low *NGDR* values for individuals in their respective groups. These correspond to Figures 5.20 and 5.22, where the individuals clearly stay in a stationary cluster. The swarm (from Figure 5.21) and the two alignment models have higher *NGDR*'s, indicating that individuals travel in relatively straight paths. An analysis of variance (ANOVA) analysis indicates strongly that there is a significant difference between the five models (logit link function).

A cohesive model has high *NGDR*'s, comparable with the values from the alignment models. This cohesive model corresponds to a swarm formation, where individuals pay no attention to other group members and move independently. This fact is reflected in Figure 5.38, which shows that the swarming group has low polarisations. Both alignment models have consistently high polarisations, over the time of the simulation.

We calculate the *NGDR*'s for the centre of the group (2.1) over the time period of the simulation. The *NGDR* of the centre of the group in the alignment model (0.9968) is substantially larger than the *NGDR* of the centre in the cohesive model (0.0533). These individual trajectories are shown in Figures 5.24 and 5.20, respectively. This indicates the former group (as a single entity) has travelled in a linear fashion over the duration of the simulation, the latter group has not. The swarm configuration (Figure 5.21) has high individual *NGDR*'s (Figure 5.37), but the group centre has a *NGDR* of 0.0280. The swarm group is not travelling as an entity, despite individuals having linear paths.

The high polarisations and *NGDR* values for the alignment model (movements shown in Figure 5.24) is indicative of an organised group,

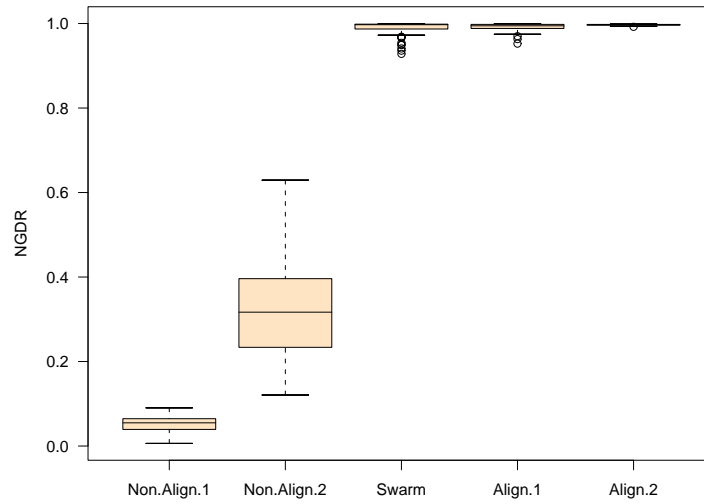


FIGURE 5.37. Boxplots of the net to gross displacement ratio ($NGDR$) for the five models. The labels are identical to Figure 5.36.

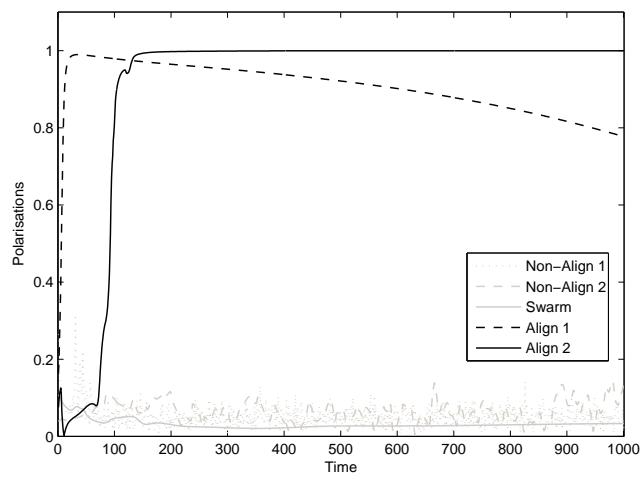
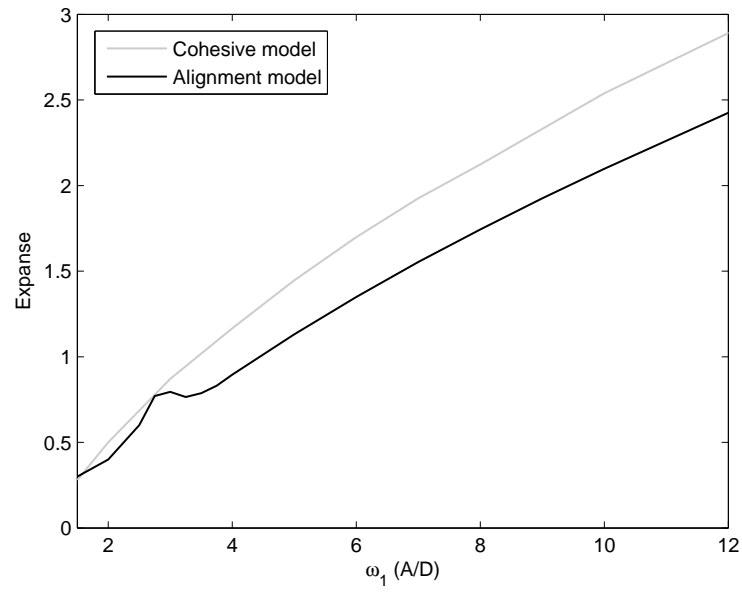
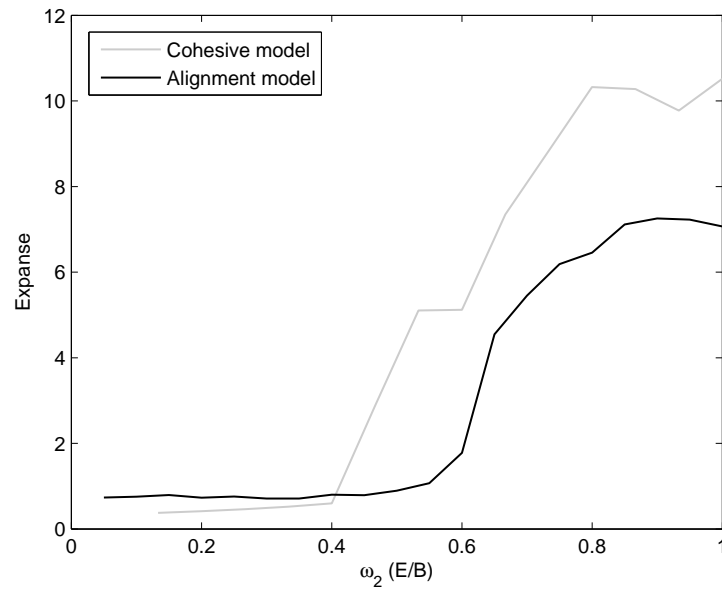


FIGURE 5.38. Polarisation resulting from the five models. The labels are identical to Figure 5.36.

FIGURE 5.39. Expanse as a function of the ratio ω_1 (A/D).FIGURE 5.40. Expanse as a function of the ratio ω_2 (E/B).

travelling in a clearly defined direction. Notice in Figure 5.38, one group has a monotonically decreasing trend to its polarisations (‘Align 1’ group, whose movements are shown in Figure 5.23). Alignment forces are present, but cohesive forces are reduced in this model, resulting in oscillations in group member’s trajectories. These oscillations cause the decrease in polarisations observed in Figure 5.38.

While individuals in the swarm group travel in relatively straight paths, these paths are not aligned with one another. The other cohesive models certainly do not travel as a coherent group, settling in a stationary cluster. Hence, we conclude that cohesive forces alone are not adequate to induce individuals to travel, although these individuals may move separately in a disorganised group. Alignment forces are required to induce travel.

Group size is (generally speaking) larger for the model with cohesive forces, in comparison to the model with alignment terms. The addition of alignment forces must produce a minor attractive effect. This trend is illustrated in Figures 5.39 and 5.40. Both types of models show a similar rate of increase in group size (as measured by expanse), as the appropriate ratios increase.

5.4. Summary

Chapters 3 and 4 involved Lagrangian aggregation models based on an individual’s response to discrete spherical social zones. We changed the approach in this chapter and introduced a potential model for collective motion, based on principles from physical mechanics and particle physics. We reinterpreted the forces resulting from these physical models as social forces, where individuals in the model experience these social forces acting upon themselves as a force field and act accordingly. These social forces act on an individual’s velocity, unlike previous models in literature. Cohesive and alignment forces are based on gradient forces, individuals follow the gradient of the corresponding potential.

Mogilner et al. (2003) developed an attractive-repulsive model based on gradient forces. The forces in their cohesive model act on the positions of the individuals. The authors update the individuals' current position by calculating the velocity due to social forces and consequently, the distance (and direction) covered by the individuals in that timestep. This is the same approach as the models in Chapters 3 and 4 (see (3.5), which is the same idea).

However, for the alignment potential model, we require the forces to act directly on the velocities. To maintain consistency, we keep this convention when considering the cohesive potential model. The potential model is designed to operate in three-dimensions and includes a term to cause group travel, we simplify by assuming radial symmetry. Mogilner et al. (2003) only consider models in one- and two-dimensions, but their analytical results generalise to higher dimensions.

Attraction and repulsion forces are included in the potential model, modelled as exponentially decaying functions. We argue that in order to generate biologically plausible behaviour, we require repulsion to be a short range force and attraction forces to dominate at medium and longer ranges. Mogilner et al. (2003) demonstrate in detail these relationships. Consequently, we show that the parameters in the cohesive models have the following relationships: $A \geq D$ and $B \geq E$.

We introduced an alignment force to the potential model to allow individuals to orient to one another. The size of this force decays, this rate of decay is based on an individual's relative distance to its neighbours. This alignment force is shown to be crucial to cause the group to travel as an entirety. We also show that a dissipative force or some other modification is essential to prevent escapes.

The role the parameters play in the cohesive and alignment models is investigated. The attraction and repulsion magnitudes directly contribute to the size of the groups formed. As the attraction magnitude

increases, the individuals experience more attractive forces and a cluster results. Conversely, as the repulsion magnitude increases, the group becomes more diffuse. The attraction and repulsion ranges control the spread of these forces. As the attraction range increases in size, the spread of the attraction force decreases exponentially and individuals tend to experience less neighbours to be attracted to. Consequently, the group tends towards swarm behaviour. Similar reasoning occurs to see that an increasing repulsion range results in clusters; repulsion forces decrease exponentially and individuals can move closer to one another.

The alignment magnitude controls the size of the alignment effect. Lower alignment magnitudes result in a model similar to the cohesive model, a transition to a travelling cluster appears approximately at values of 0.15-0.2 for the alignment magnitude. Only small friction coefficients (and therefore, small dissipative forces) are required to successfully prevent individual escapes within the potential model.

The potential model predicts that given sufficiently strong attraction forces, the resulting behaviour will be a stable sedentary cluster. Swarming behaviour results as these forces decrease. The potential model also suggests that the alignment terms are crucial to inducing the group of individuals to travel. Cohesive forces alone are not adequate. Alignment forces have a minor attractive effect, but without these forces, the individuals settle in a sedentary cluster. Frictional forces appear to be critical to curb escapees. The model predicts that an alignment force, coupled with a small frictional force and a small attraction range (compared to a larger repulsion range) will result in inducing the group of particles to travel as an entity in its own right.

We do not consider the addition of a stochastic force, as the model presented in this chapter already inherently chaotic. Stochastic components would overly complicate matters and interfere with possible Eulerian formulations.

Modelling insects as particles is a reasonable assumption for smaller insects. This potential model is applicable for small insects, like honeybees or midges. Insects like desert locusts (*Schistocerca gregaria*) have a more obvious elongated body shape, with sensory appendages located on the head and along the hairs of the back legs, the latter being a particularly important behavioural trigger (Simpson, Despland, Hägele & Dodgson 2001). These types of insects have a more obvious inhomogeneity in their perceptive field, the potential model's assumption of radial symmetry may not be valid in this case.

Mogilner et al. (2003) use Liapunov functions, designed to establish energy minima that correspond to stable stationary states of their two-dimensional cohesive model. Theoretically, we could do this to our potential model, but with the addition of alignment forces, an analytical solution becomes difficult. Numerically obtained Liapunov 'landscapes' are produced in Mogilner et al. (2003), for visual confirmation of stable equilibriums in their cohesive model. Future work could produce such graphs for our three-dimensional cohesive model to establish stable energy states, although we have three dimensions to contend with (rather than two).

This potential model is currently in a Lagrangian formulation. Work in the future involves transforming to a Eulerian formulation and taking advantage of Hamiltonian mechanics. To do this, we need to remove the friction force and replace it with a gradient force, to prevent escapes. This gradient force will work at longer ranges than the repulsion and attraction forces in Section 5.2 and should not be dependent on inter-individual spacings, but the distance between the individual and the group (perhaps, the group centre). As an escapee moves beyond the confines of the group, this individual experiences an exponential or power law increasing force, encouraging the escapee to rejoin the group. Once this has been implemented and the model has been converted to

a Hamiltonian system, we can use a large array of mathematical and physical theory has been developed in classical and quantum mechanics for such systems. This could be harnessed to advance knowledge involving this type of model used for collective motion.